

Passivation and stress corrosion cracking tendency of manganese stainless steels

A. DEVASENAPATHI, R. C. PRASAD*, V. S. RAJA
*Corrosion Science and Engineering Programme, and * Department of Metallurgical Engineering and Materials Science, Indian Institute of Technology, Bombay 400 076, India*

Stress corrosion cracking (SCC) behaviour of three grades of nickel-substituted manganese stainless steels have been studied at room temperature in 1 M HCl under constant load at different applied potentials. Repassivation studies have also been carried out using a scratching electrode technique. Selective dissolution and film formation similar to that of films formed on alpha brass in ammoniacal solutions, were found to induce SCC in manganese stainless steels. With decrease in nickel content, these alloys were found to be highly susceptible to SCC.

1. Introduction

Stress corrosion cracking (SCC) behaviour of AISI 304 austenitic stainless steels is well known [1–6]. They undergo a transgranular mode of cracking in chloride environments. AISI 304 stainless steel contains 8–10 wt % Ni which makes this alloy considerably costlier. Attempts have been made to develop austenitic stainless steel with replacement of nickel with other austenite stabilizers such as manganese, copper and nitrogen to decrease the cost, as well to find a suitable substitute for nickel. Complete replacement of nickel leads to manganese stainless steels inferior in corrosion resistance than AISI 304 stainless steel [7]. Therefore, to optimize cost and properties, nickel substituted manganese stainless steels with varying weight percentages of nickel have been developed. Interestingly, these alloys have been found to exhibit better intergranular corrosion resistance [8] and stress corrosion cracking resistance in boiling $MgCl_2$ solution [9]. However, studies on stress corrosion cracking behaviour of these alloys are very sparse [7–11].

It is well known that stainless steels exhibit corrosion resistance by forming a thin passive film on the surface. All localized corrosion failures, such as pitting, stress corrosion cracking and corrosion fatigue, occur due to the localized breakdown of these passive films. The ability of an alloy to repassivate after the passive film breakdown determines its resistance to localized failures. Alloys susceptible to SCC have to repassivate at a particular rate [12]; otherwise they undergo general corrosion due to lower repassivation rates or show SCC resistance due to higher repassivation rates. Several attempts have been made in the past to correlate the repassivation behaviour with SCC behaviour in the case of stainless steels [13–15] and brasses [16, 17].

Repassivation studies have been carried out using different techniques, such as the electrochemical

straining electrode and scratching electrode techniques. An original bare metal surface without any film created by the scratching electrode technique represents closely the crack tip generated during SCC. Also, it is possible to eliminate errors due to hydrogen or oxygen evolution encountered in the case of electrochemical techniques, if the scratching electrode technique is employed. The present work aimed to compare the SCC behaviour of three different manganese stainless steels with AISI 304 stainless steel so that they can be considered as possible cheap alternatives. An attempt was also made to correlate the repassivation behaviour of these alloys with SCC behaviour.

2. Experimental procedure

For the present study, AISI 304 stainless steel and three different nickel-substituted manganese stainless steels of Grades 1, 2 and 3 of the composition reported earlier [9] were used. The nickel content of the manganese stainless steels was 4.7, 2.3 and 0.87 wt %, respectively, with a manganese content of around 8–9 wt %. All the alloys were solution treated in a nitrogen atmosphere for 1 h at 1100 °C and quenched in water. Potentiodynamic polarization studies were carried out using 1 cm² rectangular sheets. A copper wire soldered on one face of the sheet served as electrical contact. Cold-set was carried out with polyacrylic powder to insulate the electrical contacts and to mount the electrode. The specimens were polished to 600 grit finish with SiC paper followed by a mirror finish with lap polishing using wet alumina. Specimens were degreased in methanol, washed in distilled water and dried. Polarization studies under stressed conditions were carried out using tensile test specimens loaded at 75% of their yield strength. The specimens were insulated with silicon rubber resin delineating an area of 0.5 cm² along the gauge section of the specimen.

SCC tests were carried out with smooth flat tensile test specimens of dimensions 25 mm × 6 mm × 1 mm along the gauge section with a reduced section length of 40 mm and total length of 100 mm. The tensile test specimens were polished to 600 grit finish and stressed in a spring loaded SCC test setup. SCC tests were carried out using 1 M HCl as the test solution and the time taken for the complete fracture of the specimen was taken as the time to failure. Repassivation studies were carried out in a cell similar to that of Hagyard and Earl [18] with appropriate modifications to increase the scratching speed. A diamond tip embedded on an ebonite rod was used to effect scratching, with the help of an electrically triggered solenoid valve and pneumatic cylinder operated by pressurized nitrogen gas. A PARC 273 potentiostat operated by m352 software was used in the present study. The current transients in the form of i versus t curves, were collected at a time interval of 1.5 ms. 1 M HCl, prepared from distilled water and analytical grade reagents, was used for the present study.

3. Results and discussion

Potentiodynamic polarization curves for all four alloys in 1 M HCl are given in Fig. 1. All three nickel-substituted manganese stainless steels, except Grade 1, showed a notable shift in corrosion potential, E_{corr} , towards a more active direction in comparison with AISI 304. The shift in E_{corr} towards more negative values follows the order 304 = Grade 1 < Grade 3 < Grade 2. Although there is no considerable change in the cathodic polarization behaviour of these alloys, their anodic polarization characteristics differ markedly. Thus AISI 304 stainless steel shows a clear active passive transition behaviour with a narrow passive region. No such active passive transition or passive region is exhibited by any of the three nickel-substituted manganese stainless steels. All three manganese stainless steels showed a very subtle kink in the anodic curve similar to that of the passive region, which signifies a weak tendency of the alloys to passivate. Although it has been reported earlier [19, 20] that about 12–15 wt % Cr present in Fe–Cr alloys is adequate to give a complete passivation with enrichment of Cr_2O_3 , four to six layers thick [21], the manganese stainless steels with equal chromium contents do not exhibit such stable passivation. One of the reasons for this inadequate passivation of manganese stainless steels is the presence of more active manganese and more noble copper. Manganese being electrochemically more active, undergoes selective dissolution faster than other elements. Also copper, which is more noble, tends to redeposit on the alloy surface. This results in a thick porous passive film with lower inhibiting and passivating tendency than the thin passive film formed on AISI 304 stainless steel. This higher dissolution tendency of manganese stainless steel is clearly exhibited in the polarization curves which show that at any given potential the current density of these stainless steels is higher than that of 304 stainless steel with Grade 2 with 3 wt % Ni, showing very high current densities.

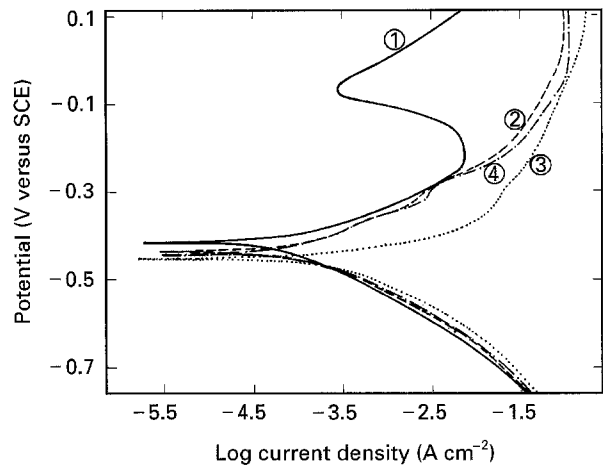


Figure 1 Potentiodynamic polarization behaviour of (1) AISI 304, (2) Grade 1, (3) Grade 2 and Grade (4) Grade 3 stainless steels in 1 M HCl.

TABLE I SCC test results of stainless steels tested at 75% of their yield strength under constant load in 1 M HCl

Potential (V versus SCE)	Time to failure (h)			
	AISI 304	Grade 1	Grade 2	Grade 3
E_{corr}	57	12	8	6.5
-0.2	14.5	11	4.5	2
0	4	3	2.5	2

SCC test results of austenitic stainless steels tested in 1 M HCl with an applied load of 75% of their yield strength are given in Table I at different applied potentials. AISI 304 shows very good SCC resistance compared to all other manganese stainless steels. Among the manganese stainless steels with decrease in nickel content SCC resistance decreases, with Grade 1 exhibiting higher SCC resistance followed by Grades 2 and 3. With increase in potential in the anodic direction, all the stainless steels fail at much lower times showing lower SCC resistance.

Repassivation curves of AISI 304 and the manganese stainless steels in 1 M HCl are given in the form of i versus t plots in Figs 2–5 in as-obtained form for an approximate scratch area of $2.4 \times 10^{-4} \text{ cm}^2$. The current obtained during repassivation (Figs 2–5) is a combination of current from the scratch and unscratched bare surface of the alloy. So the exact current passed from the scratch was obtained by subtracting the base current value from the current values obtained. The values of i_{peak} and charge density passed per square centimetre of the alloy during repassivation were calculated by dividing the current by the original scratch area, $2.4 \times 10^{-4} \text{ cm}^2$. The maximum current density reached during repassivation, i_{peak} , is a measure of the bare surface dissolution tendency of the alloy. Furthermore, based on the mechanism of anodic dissolution, the charge density passed during complete repassivation gives a measure of crack propagation rate (CPR). It has been shown by Carranza and Galvele [16] in the case of stainless steels, that it is possible to determine the crack propagation rates (CPR) from the

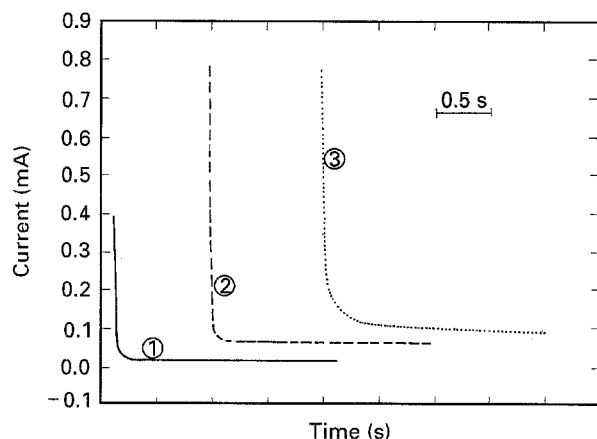


Figure 2 Repassivation behaviour of AISI 304 in 1 M HCl at (1) -0.425 V, (2) -0.2 V and (3) 0 V.

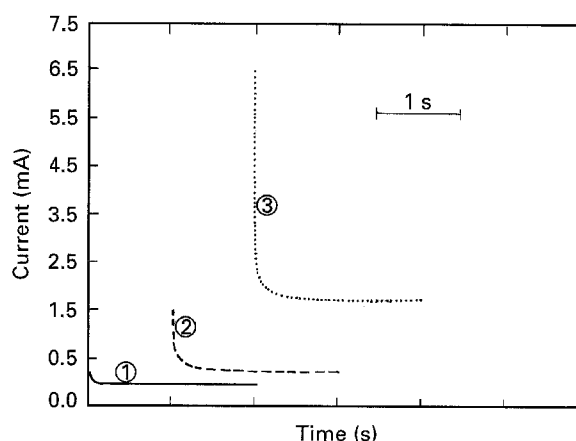


Figure 5 Repassivation behaviour of Grade 3 in 1 M HCl at (1) -0.450 V, (2) -0.2 V and (3) 0 V.

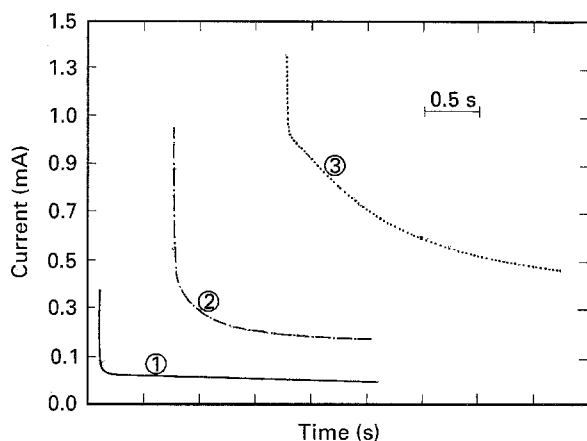


Figure 3 Repassivation behaviour of Grade 1 in 1 M HCl at (1) -0.435 V, (2) -0.2 V and (3) 0 V.

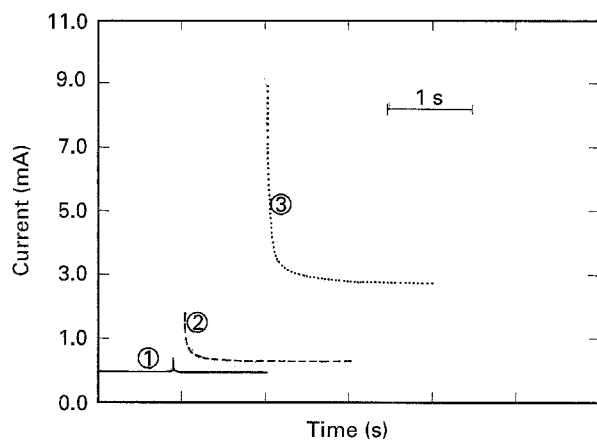


Figure 4 Repassivation behaviour of Grade 2 in 1 M HCl at (1) -0.445 V, (2) -0.2 V and (3) 0 V.

charge passed between repassivation events by using the relation

$$\text{CPR} = (M/\rho Fz)(Q_f/t_f) \quad (1)$$

where M is the atomic weight, ρ the density of the metal reacting at the crack tip, z the valence of the reacted metal, F the Faraday constant, and Q the charge density during t_f .

Repassivation study results show an increase in the i_{peak} value and the charge density passed during repas-

sivation in the case of all manganese stainless steels compared to that of AISI 304 stainless steel. In general, all the alloys exhibit an increase in current and charge density with shift in potential towards the anodic direction. AISI 304 shows i_{peak} values of 1.67, 3.1 and 3.33 A cm^{-2} and charge density values of 0.205, 0.55 and 0.751 C at potentials of -0.425 , -0.2 and 0 V versus SCE, respectively. Grade 1 exhibits i_{peak} values of 1.55, 4.35 and 5.6 A cm^{-2} and charge densities of 0.116, 1.83 and 5.35 C at potentials of -0.435 , -0.2 and 0 V versus SCE, respectively. Grade 2 exhibits i_{peak} values of 7.344 and 37.06 A cm^{-2} and charge densities of 2.98 and 24.87 C at potentials of -0.2 and 0 V versus SCE, respectively, while Grade 3 shows i_{peak} values of 7.32 and 27.04 A cm^{-2} and charge densities of 2.62 and 15.35 C at -0.2 and 0 V, respectively. At a potential of -0.4 V, Grade 2 shows a cathodic peak in addition to an anodic peak. This shows that the cathodic reaction is more favoured on the bare metal than on the filmed surface. Grade 3 also exhibits a similar trend of occurrence of cathodic reaction, though it is not so prominent as in the case of Grade 2. So the charge densities passed during repassivation could not be calculated for the Grades 2 and 3 alloys of E_{corr} . Also, with increase in potential in the anodic direction, all the alloys showed an increase in i_{peak} , charge density and base current. The increase in i_{peak} and charge density passed during repassivation follows the order $304 < \text{Grade 1} < \text{Grade 3} < \text{Grade 2}$.

SCC test results in 1 M HCl (Table I) at three different potentials show that manganese stainless steels are more highly susceptible to SCC than AISI 304 stainless steel. Also it clearly shows a trend of increased SCC susceptibility with decrease in nickel content. Grade 3 with 0.87 wt % Ni shows higher SCC susceptibility followed by Grade 2 with 2.3 wt % and Grade 1 with 4.7 wt % Ni content. While austenitic stainless steels, in general, undergo a transgranular mode of cracking under solution treatment conditions in chloride environments, all the manganese stainless steels exhibit a predominantly intergranular mode of cracking which changes into transgranular mode with increase in stress [11]. This is seen in the fractograph of Grade 1 (Fig. 6) alloy failed at E_{corr} showing an

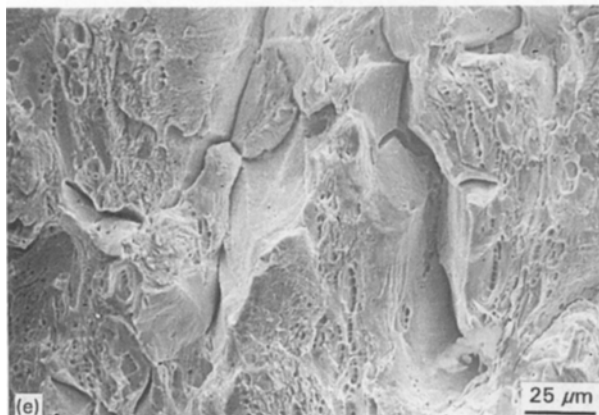
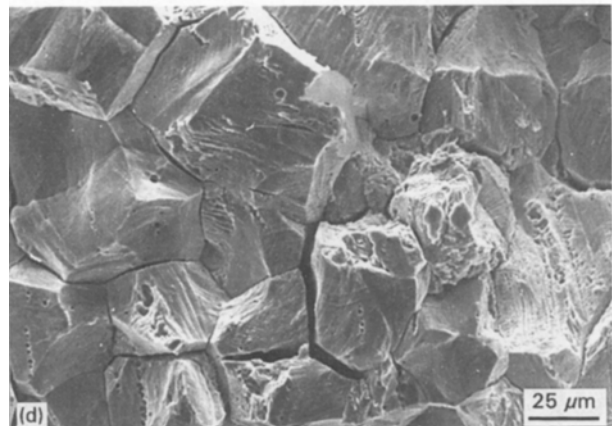
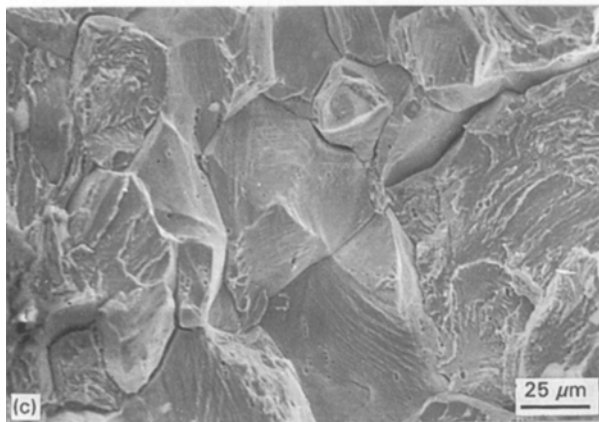
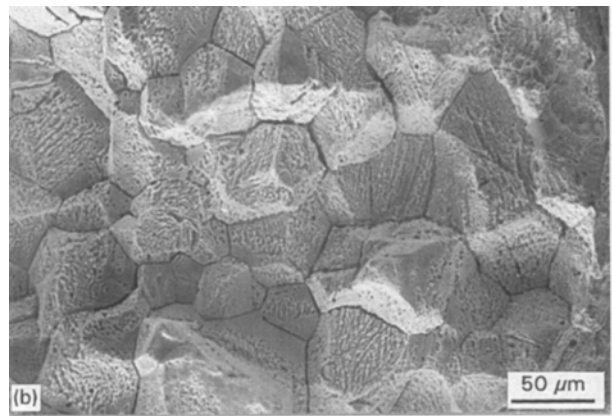
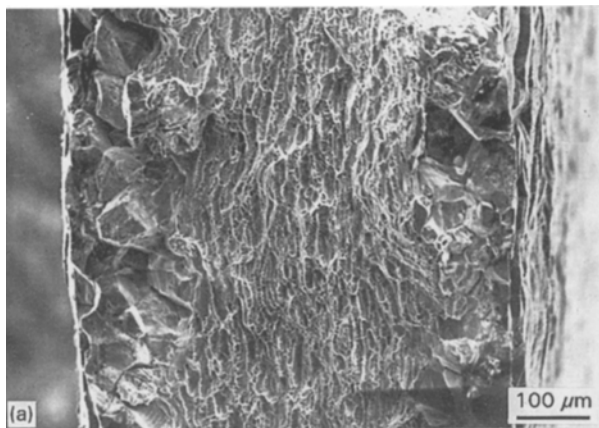


Figure 6 (a) Fractograph of Grade 1 alloy failed at E_{corr} showing an intergranular mode of cracking at the edges due to SCC and dimples in the middle portion due to a ductile overload failure by microvoid coalescence. (b) Fractograph of Grade 2 alloy failed at an externally applied potential of -0.2 V showing an intergranular mode of failure. (c) Fractograph of Grade 3 alloy failed at 0 V showing the change in fracture mode from intergranular to transgranular. (d) Fractograph of Grade 1 alloy failed at 0 mV showing a mixed mode of failure. (e) Fractograph of Grade 3 alloy failed at -0.2 V showing a mixed mode of failure.

intergranular mode of cracking at the edges due to SCC and dimples in the middle portion of the specimen showing a ductile overload failure by microvoid coalescence. The fractograph of Grade 2 alloy failed at an externally applied potential of -0.2 V shows an intergranular mode of failure as shown in Fig. 6b. The change in fracture mode from intergranular to transgranular is seen in the fractograph (Fig. 6c) of Grade 3 alloy failed at 0 V. The mixed mode of failure is further shown in fractographs of Grade 1 failed at 0 V (Fig. 6d) and Grade 3 failed at -0.2 V (Fig. 6e) in 1 M HCl. Although there is an apparent agreement among SCC, polarization and repassivation experiments in the sense that the alloy becomes more susceptible to SCC failure the higher the anodic dissolution, the higher the i_{peak} and higher is the charge density passed during repassivation, an exception has occurred in the

increasing order of susceptibility between Grades 2 and 3. That is, the Grade 2 alloy should have exhibited a lower i_{peak} , charge density and anodic current, because its susceptibility to SCC is less than that of Grade 3. This apparent contradiction can be resolved if we consider the nature and the role of film formation on the alloys.

Intense black film formation on the surface of Grades 2 and 3 stainless steels was observed, while Grade 1 with 4.7 wt % Ni showed black tinges of film formation at much later stages. Also the surfaces were found to be coated with copper. This was further confirmed by the EDAX studies [9] of the surface film formed on Grade 3 alloy in 1 M HCl which showed the enrichment of copper with depletion of iron and manganese. The SCC test specimens after failure were also found to be coated with copper. It is worthwhile

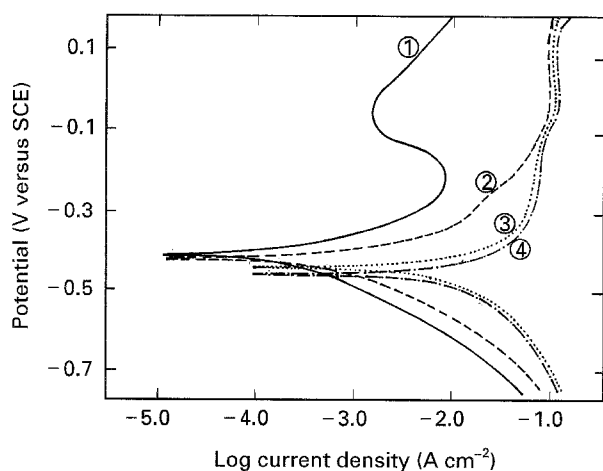


Figure 7 Potentiodynamic polarization behaviour of (1) AISI 304, (2) Grade 1, (3) Grade 2 and (4) Grade 3 stainless steels in 1 M HCl at 75% of their respective yield strengths.

mentioning that Asawa [22] also reported copper plating on the surface, when 304 stainless steel containing copper was immersed in a sulfuric acid environment due to redeposition subsequent to dissolution along with other alloying elements. Intense hydrogen evolution with this black surface film formation was noticed in Grades 2 and 3 stainless steels, indicating extensive corrosion in 1 M HCl. The electrochemical kinetics is governed by these films. On the other hand, the mechanical integrity of the thick films under applied stresses can be lost. This discrepancy observed between the SCC test results, on the one hand, and polarization, repassivation on the other, can be attributed to breaking of these thick films under applied stress and consequent changes in dissolution behaviour. The potentiodynamic polarization behaviour of the alloys under 75% of their yield strength is shown in Fig. 7. Comparison of this with the polarization curves obtained without stress (Fig. 1) shows a general increase in anodic dissolution characteristics of all the alloys under stress. Further, it is noted that the anodic dissolution current of Grade 3 alloy is increased considerably over that of Grade 2 alloy. This confirms the change in the dissolution behaviour under stress and also correlates well with its higher susceptibility observed towards SCC (Table I). So further studies are being carried out to determine the effect of applied stress on repassivation behaviour of these alloys. Another important factor that deserves attention is that while generally a decrease in nickel content is expected to reduce SCC [22] due to the reduction in stacking fault energy, a reversal was found in the present study. This may be due to film-assisted crack growth.

4. Conclusions

1. All three grades of manganese stainless steels exhibit inadequate passivation in 1 M HCl.
2. i_{peak} and charge density values obtained for manganese stainless steel during repassivation are higher than that of AISI 304 stainless steel.
3. With decrease in nickel content, SCC susceptibility of manganese stainless steels increases.
4. The SCC susceptibility increases with increase in potential in the anodic direction for all grades of stainless steels.

References

1. A. J. SEDRIKS, *Int. Met. Rev.* **27** (1982) 321.
2. H. R. COPSON, in "Physical metallurgy of stress corrosion fracture", edited by T. N. Rhodin (Interscience, New York, 1959) p. 247.
3. R. M. LATANISION and R. W. STAEHLE, in "Fundamental aspects of stress corrosion cracking", edited by R. W. Staehle, A. J. Forty and D. Von Rooyen (NACE, Houston, TX, 1969) p. 214.
4. R. W. STAEHLE, J. J. ROYUELA, T. L. RAREDON, E. SERRATE, C. R. MORIN and R. V. FARRAR, *Corrosion* **26** (1970) 451.
5. J. D. HARTSON and J. C. SCULLY, *ibid.* **26** (1970) 387.
6. G. BIANCHI, F. MAZZA and S. TORCHIO, *Corros. Sci.* **13** (1973) 165.
7. P. RAMA RAO and V. V. KUTUMBA RAO, *Int. Mater. Rev.* **34** (1989) 69.
8. V. S. RAJA and A. RAMKUMAR, *Br. Corros. J.*, in press.
9. A. DEVASENAPATHI, G. S. RAMAKRISHNA and V. S. RAJA, *J. Mater. Sci. Lett.* **14** (1995) 233.
10. DONALD WARREN, *Corrosion* **16** (1960) 101.
11. A. DEVASENAPATHI, R. C. PRASAD and V. S. RAJA, *Scripta Metall.* **33** (1995) 233.
12. J. C. SCULLY, *Corros. Sci.* **15** (1975) 513.
13. P. ENGSETH and J. C. SCULLY, *ibid.* **15** (1975) 505.
14. R. M. CARRANZA and J. R. GALVELE, *ibid.* **28** (1988) 233.
15. I. MAIER and J. R. GALVELE, *ibid.* **36** (1980) 60.
16. R. M. CARRANZA and J. R. GALVELE, *Corros. Sci.* **28** (1988) 851.
17. D. J. LEES and T. P. HOAR, *ibid.* **20** (1980) 761.
18. T. HAGYARD and W. B. EARL, *J. Electrochem. Soc.* **144** (1968) 684.
19. I. OLEFJORD, *Mater. Sci. Eng.* **42** (1980) 161.
20. *Idem*, *ibid.* **47** (1980) 173.
21. S. BOUDIN, C. BOMBART, G. LORANG and M. da CUNHA BELO, in "Modifications of passive films", European Federation of Corrosion Publication no. 12, edited by P. Marcus, B. Baroux and M. Keddad (Institute of Materials, London, 1994) p. 35.
22. M. ASAWA, *Corrosion* **46** (1990) 829.

Received 8 August
and accepted 21 December 1995